Development 117, 925-936 (1993)
Printed in Great Britain © The Company of Biologists Limited 1993

Altered rhombomere-specific gene expression and hyoid bone differentiation in the mouse segmentation mutant, *kreisler* (*kr*)

Michael A. Frohman[1,*], Gail R. Martin[1], Sabine P. Cordes[2], Louis P. Halamek[2] and Gregory S. Barsh[2]

[1]Department of Anatomy and Program in Developmental Biology, School of Medicine, University of California at San Francisco, San Francisco, CA 94143, USA
[2]Department of Pediatrics and Howard Hughes Medical Institute, Stanford University, Stanford, CA, 94305, USA

*Present address: Department of Pharmacological Sciences, SUNY at Stony Brook, Stony Brook, NY 11794-8651, USA

SUMMARY

Rhombomeres appear transiently in the vertebrate hindbrain shortly after neurulation and are thought to represent embryologic compartments in which the expression of different combinations of genes leads to segment-specific differentiation of the developing hindbrain, the cranial ganglia, and the branchial arches. To determine the extent to which gene expression is related to the formation of visible rhombomere boundaries, we have examined, by in situ hybridization, the expression of five rhombomere-specific genes in mouse embryos homozygous for the *kreisler* (*kr*) mutation, in which rhombomeres 4-7 are replaced by a smooth morphologically unsegmented neural tube.

Using molecular probes specific for *Hoxb-1 (Hox-2.9)*, *Hoxb-3 (Hox-2.7)*, *Hoxb-4 (Hox-2.6)*, *Krox-20*, or *Fgf-3* (*Int-2*), we found that the *kr* mutation affects the expression of all the genes we examined, but, surprisingly, the altered patterns of expression are not restricted to that portion of the mutant hindbrain which is morphologically abnormal. Rostral expression boundaries of *Hoxb-3* and *Hoxb-4* are displaced from their normal positions at r4/5 and r6/7 to the approximate positions of r3/4 and r4/5, respectively. The expression domains of *Krox-20* and *Fgf-3* are also displaced in a rostral direction and the intensity of *Fgf-3* hybridization is greatly reduced. The expression domain of *Hoxb-1* is affected differently from the other genes in *kr*/*kr* embryos; its rostral boundary at r3/4 is intact but the caudal boundary is displaced from its normal location at r4/5 to the approximate position of r5/6. Because boundaries of gene expression for *Hoxb-1* and *Hoxb-4* are found in a region of the *kr*/*kr* hindbrain that lacks visible rhombomeres, establishment of regional identity, as reflected by differential gene expression, does not require overt segmentation.

To investigate whether the altered patterns of gene expression we observed in the *kr*/*kr* embryonic hindbrain are associated with morphologic changes in the adult, we examined neural crest-derived tissues of the second and third branchial arches, which normally arise from rhombomeres 4 and 6, respectively. We found that the hyoid bone in *kr*/*kr* animals exhibited an accessory process on the greater horn (a third arch structure) most easily explained by ectopic development of a second arch structure (the hyoid lesser horn) in an area normally derived from the third arch.

Key words: rhombomere, hindbrain development,homeobox, Hox gene expression,kreisler, branchial arch, hyoid bone, *Krox-20*, *Fgf-3*, mouse

INTRODUCTION

Embryonic segmentation is an evolutionarily conserved developmental strategy used to build and to diversify different body regions. During vertebrate hindbrain development, the neural plate transiently divides into seven segments (rhombomeres) that differentiate according to their position along the rostrocaudal axis (reviewed by Keynes and Lumsden, 1990). Although the mechanisms responsible for rhombomere formation are not understood, several lines of evidence suggest that rhombomeres represent developmental compartments. Cell lineage and cell tracer analyses have shown that rhombomere boundaries denote limits of cell migration (Fraser et al., 1990), and that adult derivatives of rhombomeres — sensory ganglia, motor nerve roots, and branchial arch-derived structures — exhibit a segmental organization consistent with their particular rhombomeric origins (Lumsden and Keynes, 1989; Lumsden et al., 1991). In addition, individual rhombomeres are characterized by the expression of different combinations of genes (reviewed by Wilkinson and Krumlauf, 1990), including *Hox* genes and other putative transcription factors such as *Krox-20* (Murphy et al., 1989; Wilkinson et al., 1989a,b; Frohman et al., 1990), and secreted signalling molecules such as that encoded by the *Fgf-3* gene (previously known as *Int-2*; Wilkinson et al., 1988). These genes may have a role in segment formation, in determining the fate of rhombomere derivatives, or in inductive interactions

between the hindbrain and nearby tissues (Wilkinson et al., 1989b; Hunt et al., 1991c; Represa et al., 1991; Guthrie et al., 1992).

The analysis of mouse mutations is an established approach for investigating the genetic control of mammalian developmental pathways. The *kreisler* (*kr*) mutation, first identified by its effects on auditory and vestibular function in the adult, was subsequently found to alter the pattern of rhombomere formation in the developing hindbrain (Hertwig, 1942a,b; Deol, 1964). In *kr*/*kr* embryos, the first three rhombomeres appear normal, but r4-r7 are replaced by a smooth, morphologically unsegmented neural tube. The adjacent neural crest, which normally appears to emanate from r2, r4, and r6, instead appears as a continuous sheet extending caudally from the junction of r3 and r4. In addition, the position of the developing otic vesicle is shifted from its normal location near the junction of r5 and r6 to a more lateral location, and is separated from the neural tube by preganglionic neural crest (Deol, 1964). Subsequent formation of the endolymphatic duct and differentiation of sensory epithelium in the membranous labyrinth is absent or rudimentary in *kr*/*kr* embryos, so that a normal inner ear is never formed. A tendency for unrestricted expansion of the abnormal otic vesicle often produces a cyst that impinges on the hindbrain and/or middle ear structures (Hertwig, 1944; Deol, 1964). However, despite the abnormal position of neural crest in the mutant hindbrain, there are no obvious craniofacial defects in adult animals other than those produced by a cystic otic vesicle. Deafness and loss of vestibular function in adult *kr*/*kr* animals are associated with a characteristic phenotype of circling and head-tossing similar to that seen with other mutations that affect the inner ear.

The disturbance of caudal hindbrain development in *kr*/*kr* embryos offers the opportunity to investigate the relationship between rhombomere formation, spatially restricted gene expression, and segment-specific differentiation. We have examined the expression domains of *Hoxb-4*, *b-3*, *b-1*, *Krox-20*, and *Fgf-3* in the hindbrain of *kr*/*kr* and *kr*/+ embryos. (*Hoxb-4*, *b-3*, and *b-1* were previously known as *Hox-2.6*, *Hox-2.7*, and *Hox-2.9*, respectively). These genes are normally expressed in discrete areas of the neurectoderm, including that portion affected by the *kr* mutation. We find spatially restricted gene expression in the absence of visible rhombomere formation. Surprisingly, all but one gene exhibit forward displacement of their normal expression domains, suggesting that the *kr* mutation disturbs the acquistion of positional identity along the rostrocaudal axis. To determine if these abnormal patterns of gene expression are correlated with abnormalities in segmental differentiation, we examined bony and cartilaginous structures of the branchial arches. These structures are formed by neural crest cells that carry a form of prepatterning acquired during neural tube segmentation. In *kr*/*kr* animals, we find a malformation that is consistent with ectopic development of a second arch structure in the third branchial arch.

MATERIALS AND METHODS

Mouse strains and mutations

Mice carrying the *kr* mutation were obtained as double heterozygotes for *kr* and the *non-agouti* (*a*) coat color locus, *a kr*/*A* +. Homozygous *kr*/*kr* animals exhibit reduced viability between birth and weaning and female homozygotes are usually sterile. We are establishing a congenic strain on a C3H/HeJ background; heterozygotes used in the current study were between the second and tenth generation of inbreeding. All mice were obtained originally from The Jackson Laboratory, Bar Harbor, Maine.

Genotypic identification of *kr*/*kr* embryos

Embryos were obtained from naturally mated *a Emv-15*^{a} *kr*/*a Emv-15*^{a} *kr* males and *a Emv-15*^{a} *kr*/*A Emv-15*^{b} + females at E9.5, assuming the day of copulatory plug appearance as E0.5. The *Emv-15*^{b} allele is marked by a *Hin*dIII site 2.6 kb away from the proviral insertion site; this *Hin*dIII site is absent from the *Emv-15*^{a} allele (Fig. 1). The *kr*/*kr* embryos were identified as those homozygous for E*mv-15*^{a}/*Emv-15*^{a}.

The visceral yolk sac of each embryo was placed in 10 μl of water and incubated at 100°C for 5 minutes. Half of the material was used as a substrate for enzymatic DNA amplification by the polymerase chain reaction (PCR) for 40 cycles using *Taq* DNA polymerase and the oligonucleotide primers 5′-CATTCTTGAGGGCTATTGAGGTACC-3′ and 5′-CAGAGTATTGGATATTGTCATGACCC-3′, using denaturation, annealing, and extension periods of 94°C/1 minute, 60°C/1 minute, and 72°C/30 seconds, respectively. An aliquot of the amplified material was digested with *Hin*dIII and electrophoresed on a 1% agarose gel, which was then stained with ethidium bromide to determine whether the *Hin*dIII site associated with *Emv-15*^{b} was present.

DNA probes

Probes used to examine the expression of *Hoxb-3* and *Krox-20* were isolated by PCR based on the published sequences. Both probes correspond to 3′ untranslated regions; the *Hoxb-3* probe is 534 bp in length (residues 666-1199; Graham et al., 1988); the *Krox-20* probe is 1005 bp in length (residues 1796-2800; Chavrier et al., 1988). To obtain a 3′ untranslated probe specific for *Hoxb-4*, we used a PCR technique for cloning unknown cDNA ends (Frohman et al., 1988). A fragment 1100 bp in length was obtained, starting at bp 173 of the homeobox (Graham et al., 1988).

Probes used to examine the expression of *Hoxb-1* and *Fgf-3* have been described previously; the *Hoxb-1* probe is 637 bp in length (residues 889-1526; Frohman et al., 1990); the *Fgf-3* probe is approximately 1300 bp in length (pInt-2 C.28; Mansour and Martin, 1988).

In situ hybridization

In situ hybridization of embryos embedded in paraffin was performed as previously described using ^{35}S-labelled RNA probes (Frohman et al., 1990). Control hybridizations with sense probes showed no specific hybridization. The sections shown in Figs 2 and 3 are representative of the approx. 3000 serial sections examined from 18*kr/kr* and 20 *kr/+* littermates.

Morphological studies

Differential staining of bone and cartilage in embryonic mouse skeletons was performed with alcian blue and alizarin red (Inouye, 1976; McLeod, 1980). After fixation in 95% ethanol and removal of skin, viscera, and excess fat, skeletons were placed in a solution of alcian blue and alizarin red for a minimum of 3 days. The specimens were then cleared through graded dilutions of 1% potassium hydroxide and glycerol. Hyoid bones were then isolated and stored in glycerol before being photographed. Adult skeletons were prepared in a similar manner except that the initial

fixation was performed in formaldehyde. For some adult specimens, residual connective tissue was removed by a 5-60 minute incubation in 10 μg/ml proteinase K at 37°C.

RESULTS

Identification of *kr*/*kr* and *kr*/+ embryos by the use of a closely linked molecular marker

The *kr* mutation is completely penetrant in newborn animals, but mutant and non-mutant embryos are not easily distinguished solely by their external appearance. We therefore developed an unambiguous method of genotypic identification based on inheritance of a closely linked polymorphic *Hin*dIII site immediately flanking the *Emv-15* locus (Lovett et al., 1987; Siracusa et al., 1987). Genetic mapping experiments have shown previously that *kr* and *Emv-15* are each closely linked to the *non-agouti* (*a*) coat color locus (by 0.7±0.7 recombination units [*Emv-15*, *a*; Siracusa et al., 1989] and 0.97±0.32 recombination units [*kr*, *a*; Davisson et al., 1989]), but the gene order in this region was not known. In intercross and backcross experiments informative for *a*, *kr*, and *Emv-15*, we examined the segregation of *Emv-15* using oligonucleotide primers flanking the nearby *Hin*dIII site. There were no recombinants between *Emv-15* and *kr* among 85 progeny informative for 93 meioses; and a single recombinant was found between *a* and *Emv-15* among 66 progeny informative for 69 meioses (Fig. 1, Table 1). These data indicate that the gene order is *a* - (*Emv-15*, *kr*), and that *Emv-15*, as detected by the *Hin*dIII polymorphism, is sufficiently closely linked to *kr* to serve as a reliable marker for the inheritance of the mutant allele. Therefore, in the in situ hybridization experiments described below, inheritance of *Emv-15*^{a} in embryos derived from a *a Emv-15*^{a} *kr*/*a Emv-15*^{a} *kr* × *A Emv-15*^{b} +/*a Emv-15*^{a} *kr* cross was used to distinguish mutant and non-mutant embryos.

Expression of *Hoxb* genes in *kr*/*kr* and *kr*/+ embryos

Subdivision of the hindbrain into rhombomeres becomes apparent around 8.5 days of development (E8.5) as regional differences in cell proliferation produce an outward curvature in the middle of each segment (the neuromeric sulci) and as preferential axon outgrowth along parallel arrays of cytoskeletal elements causes visible boundaries (the interneuromeric gyri) to form between adjacent rhombomeres (Tuckett et al., 1985; Tuckett and Morriss-Kay, 1985; Lumsden and Keynes, 1989; Wilkinson et al., 1989b). We first investigated whether the absence of visible r4/5, r5/6, and r6/7 boundaries in *kr*/*kr* embryos is associated with altered expression of *Hoxb* genes, whose expression domains normally lie in this area. In order to accomplish this, serial sections of *kr*/+ and *kr*/*kr* embryos at E9.5 were hybridized with probes for *Hoxb-1*, *b-2*, and *b-3*, whose rostral limits of expression in normal embryos are found at the r3/4, r4/5 and r6/7 boundaries, respectively (Murphy et al., 1989; Wilkinson et al., 1989b; Frohman et al., 1990; see also Fig. 2). A total of 20 *kr*/+ and 18 *kr*/*kr* embryos were examined. Figs 2A and B illustrate the morphology of a typical *kr*/+ and a *kr*/*kr* embryo, respectively. The distinguishing features, readily apparent here, are the absence in the *kr*/*kr* embryo of distinct rhombomere boundaries caudal to the r3/4 boundary and the lateral displacement of the otocyst.

The expression pattern of the *Hoxb-1* gene in the developing embryo is well documented. This gene is exceptional among *Hox* genes expressed in the hindbrain in that it normally exhibits both a sharp rostral and a sharp caudal limit of expression. These limits coincide with the r3/4 and r4/5 boundaries, such that, in +/+ embryos, *Hoxb-1* expression in the hindbrain is restricted to r4. Moreover, *Hoxb-1* RNA levels appear to be uniformly high throughout the normal expression domain. This same pattern of expression is observed in *kr*/+ embryos (Fig. 2C). However, in *kr*/*kr*

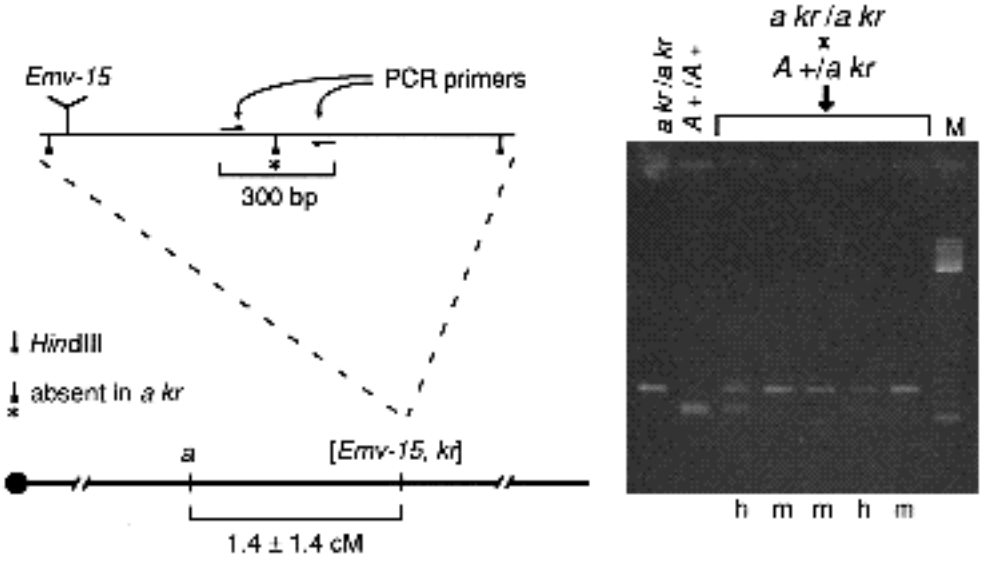

Fig. 1. Genotypic identification of *kr*/*kr* embryos by their inheritance of a closely linked restriction fragment length variant at the *Emv-15* locus. The left panel illustrates the relative map positions and distances of *a*, *Emv-15*, and *kr*. A *Hin*dIII site 2.6 kb distant from the insertion site of *Emv-15* is absent from *a kr* chromosomes (*Emv-15*^{a}) and present on *A* + chromosomes (*Emv-15*^{b}). Oligonucleotide primers flanking this variant *Hin*dIII site were used to amplify genomic DNA via the polymerase chain reaction (PCR) from visceral yolk sac tissue of each embryo. Inheritance of the variant *Hin*dIII site distinguishes homozygous mutant (m) from heterozygous (h) embryos, as shown in the right panel. Controls include amplified genomic DNA of *a kr*/*a kr* and *A* +/*A* + animals, and a 123 basepair ladder as size marker (M).

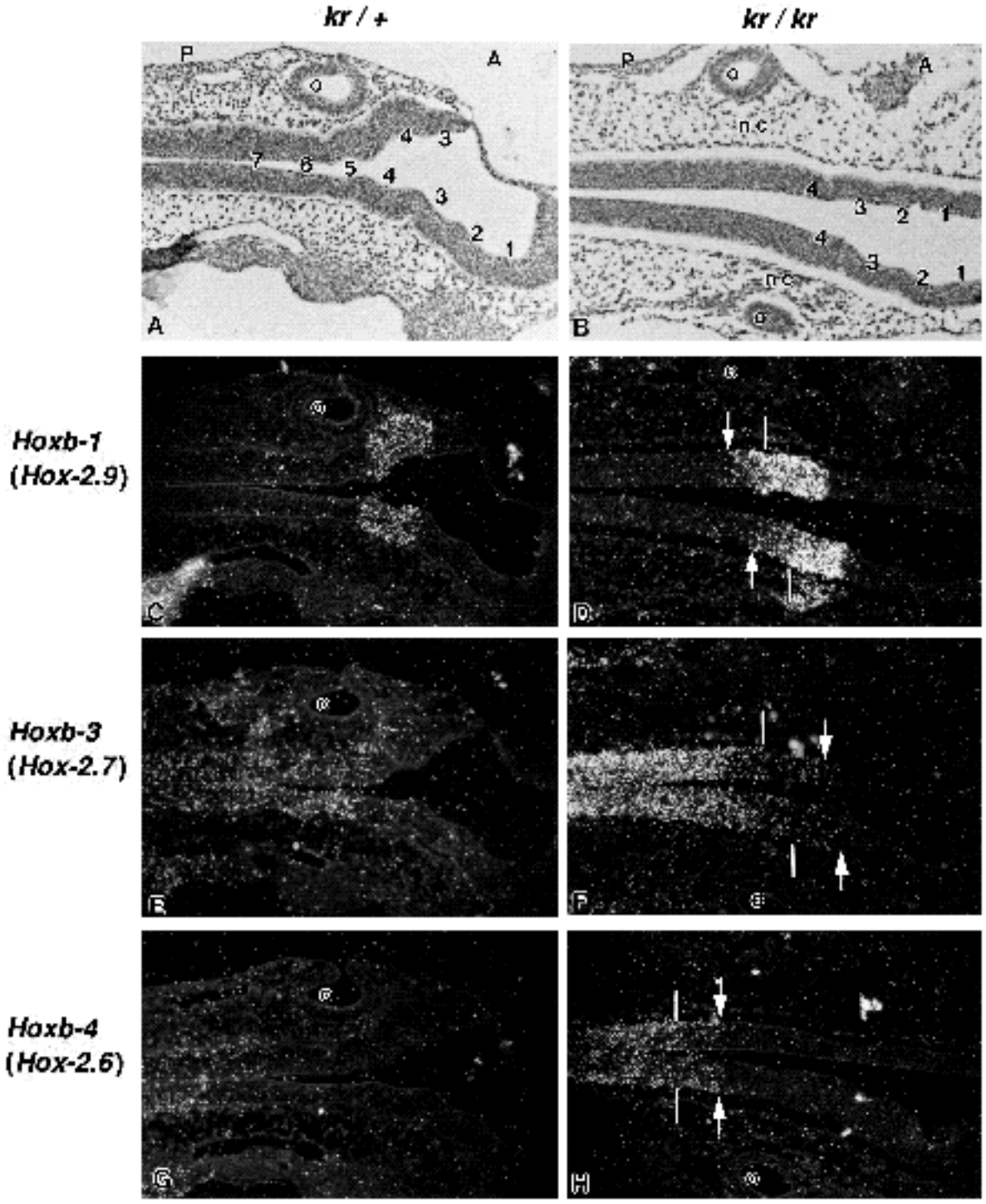

Fig. 2. Expression of *Hoxb* genes in *kr*/+ and *kr*/*kr* embryonic hindbrains. The patterns of expression of *Hoxb* genes in the hindbrain of *kr*/+ (left column) and *kr*/*kr* (right column) embryos (E9.5) were determined by in situ hybridization of serial coronal sections. The bright-field images (A,B) are each representative of the set of serial sections hybridized with probes for *Hoxb-1* (C,D), *Hoxb-3* (E,F), and *Hoxb-4* (G,H), shown beneath (dark-field images). Rhombomeres are numbered, except in the posterior part of the *kr*/*kr* hindbrain where rhombomere boundaries are not visible. Vertical bars indicate where the limit of the normal expression domain would presumably be found, and vertical arrows indicate the limit of the abnormal *Hox* gene expression domain in *kr*/*kr* embryos. A, anterior; nc, neural crest; o, otocyst; P, posterior. Magnification: ×80.

embryos the domain of *Hoxb-1* expression is altered in several respects (Fig. 2D). First, although the rostral limit of expression appears normal, the caudal limit of expression is not sharp. Second, the length of the expression domain appears to be increased. Since the rostral limit of *Hoxb-1* expression coincides with the morphologically normal r3/4

Table 1. Segregation of *a*, *Emv-15*, and *kr*

Crosses*	Characteristics of offspring: coat color	*kreisler* (behavior)	*Emv-15* genotype *a / a*	*a / b*	*b / b*
Intercross:	agouti (*A/a* or *A/A*)	non-mutant (*kr*/+ or +/+)	0	30	12
	agouti	mutant (*kr/kr*)	1	0	0
a Emv-15^a *kr* / *A Emv-15*^{b} + ×	non-agouti (*a/a*)	non-mutant	0	0	0
a Emv-15^a *kr* / *A Emv-15*^{b} +	non-agouti	mutant	2	0	0
	N.D.†	non-mutant	0	11	7
	N.D.	mutant	5	0	0
	Total	non-mutant	0	41	19
		mutant	8	0	0
Backcross:	agouti	non-mutant	0	53	
a Emv-15^a *kr*	agouti	mutant	0	0	
a Emv-15^a *kr* ×	non-agouti	non-mutant	0	0	
	non-agouti	mutant	10	0	
a Emv-15^a *kr* / *A Emv-15*^{b} +	N.D.	non-mutant	0	13	
	N.D.	mutant	1	0	
	Total	non-mutant	0	66	
		mutant	11	0	

Recombination frequency*:
(*Emv-15*, *kr*) = 0/93; c ≤ 3.1
(*a*, [*Emv-15*, *kr*]) = 1/69 = 1.4±1.4

*Genotypes of *a kr* / *a kr* parental animals were determined by coat color and behavior. *A* + /*a kr* parental animals were F_1 progeny of *a kr* / *a kr* × *A* + / *A* + matings.

†Because some parental animals were heterozygous for the *c* mutation, a proportion of albino offspring (*c*/*c*) were produced from each cross, and in these animals, the agouti genotype could not be determined from the coat color.

‡Recombination frequency, c, is calculated according to Green (1981). For recombination between *Emv-15* and *kr*, all of the 77 backcross progeny could be scored, but only 8 intercross progeny (those that were *Emv-15*^{a} *kr* / *Emv-15*^{a} *kr*) could be scored, giving a total of 93 meioses (77 + [8 × 2]). The upper 95% confidence limit for c is 3.1. For recombination between *a* and (*Emv-15*, *kr*), 63 backcross progeny could be scored, but only 3 of the intercross progeny (those that were *a*/*a* or *kr*/*kr*) could be scored, giving a total of 69 (63 + [3 × 2]) meioses.

boundary, it follows that the limit of the expression domain is more caudal than in *kr/+* embryos, possibly at a position equivalent to that of the normal r5/6 boundary. Finally, RNA levels are not uniform, but instead appear to be significantly reduced in the caudal part of the expression domain. This leads us to suggest that in *kr/kr* embryos, there is ectopic expression of *Hoxb-1* in a region that may be the equivalent of r5, but that the level of expression is reduced compared to that in r4.

We next examined the expression of the *Hoxb-3* gene at E9.5. It was previously reported that the rostral limit of expression of this gene coincides with the r4/5 boundary (Wilkinson et al., 1989b), although recent studies have indicated that a subset of *Hoxb-3* transcripts are expressed in a domain with a more rostral limit, at the r2/3 boundary (Sham et al., 1992). Under the conditions of hybridization we employed, the rostral limit of *Hoxb-3* expression was found at the r4/5 boundary in *kr/+* embryos, and no hybridization signal above background level was detected in more rostral regions of the neural tube (Fig. 2E and data not shown). However, in *kr*/*kr* embryos, we found that the rostral limit of *Hoxb-3* expression was shifted forward by one rhombomere length to the readily visible r3/4 boundary. Notably, *Hoxb-3* RNA levels were significantly lower in the area equivalent to r4 and r5, in which *Hoxb-3* and *Hoxb-1* are both expressed in *kr*/*kr* embryos (Fig. 2F). In agreement with studies on +/+ embryos, the *Hoxb-3* expression domains in *kr*/+ and in *kr*/*kr* embryos displayed no caudal limit within the hindbrain.

As previously described for +/+ embryos, the *Hoxb-4* gene in *kr*/+ embryos is expressed in a domain that extends rostrally to the r6/7 boundary and has no caudal limit in the hindbrain (Graham et al., 1988; Gaunt et al., 1989; Wilkinson et al., 1989b; Fig. 2G). In *kr/kr* embryos, however, the *Hoxb-4* expression domain extends to a rostral limit within the caudal hindbrain where there is no visible rhombomere boundary (Fig. 2H). The rostral limit of *Hoxb-4* expression is normally separated from the caudal limit of *Hoxb-1* expression by a 2 rhombomere gap, but in *kr*/*kr* embryos, analysis of serial sections hybridized with the probes for *Hoxb-4*, *Hoxb-3*, or *Hoxb-1* revealed that the rostral limit of *Hoxb-4* expression coincided with the caudal limit of *Hoxb-1* expression (Fig. 2D,F,H, and data not shown). As discussed above, the domain of *Hoxb-1* expression in *kr*/*kr* embryos is increased caudally by approximately 1 rhombomere length. Thus, the rostral limit of *Hoxb-4* expression appears to be shifted forward by one rhombomere length in *kr/kr* embryos, as was the case for *Hoxb-3*. However, in contrast to what was observed for *Hoxb-3*, the level of *Hoxb-4* RNA appears to be relatively uniform throughout the expression domain.

Expression of *Krox-20* and *Fgf-3* in *kr*/*kr* and *kr*/+ embryos

The *Krox-20* gene, which encodes a DNA-binding protein and putative transcription factor unrelated to those encoded by *Hox* genes, is also expressed in areas of the hindbrain affected by the *kr* mutation. Between E8.0 and E10.0, the expression pattern of *Krox-20* in +/+ embryos undergoes a number of changes**.** Initially, *Krox-20* RNA is detected only in r3; subsequently, expression is observed in r3 and r5, and by E9.5 it is limited to r5 alone (Wilkinson et al., 1989a; Murphy and Hill, 1991). Similarly, we found that in *kr*/+ embryos at E9.5, high levels of *Krox-20* RNA were observed in r5, but none was detectable above background levels in r3 (Fig. 3E and data not shown). However, in *kr*/*kr* embryos at the same stage of development the pattern of *Krox-20* expression was reversed. Using morphological features and hybridization with the *Hoxb-1* probe as markers for the region corresponding to rhombomeres 4 and 5 (Fig. 3B,D), we could not detect *Krox-20* RNA in r5, but low levels of expression were detectable in r3. (Fig. 3F and data not shown). We think it unlikely that this observation is due to altered timing of the events responsible for restricted expression of *Krox-20*, because among the 18 *kr*/*kr* embryos examined at E9.5, there was variation in developmental maturity corresponding to approximately 0.5 days of gestation, and in none of these *kr*/*kr* embryos was expression of *Krox-20* detected in the region representing r5. Instead, we suggest that, like the alterations in the rostral limits of *Hoxb-4* and *Hoxb-3* expression, *Krox-20* expression in r3 of *kr*/*kr* embryos represents a rostral displacement of the

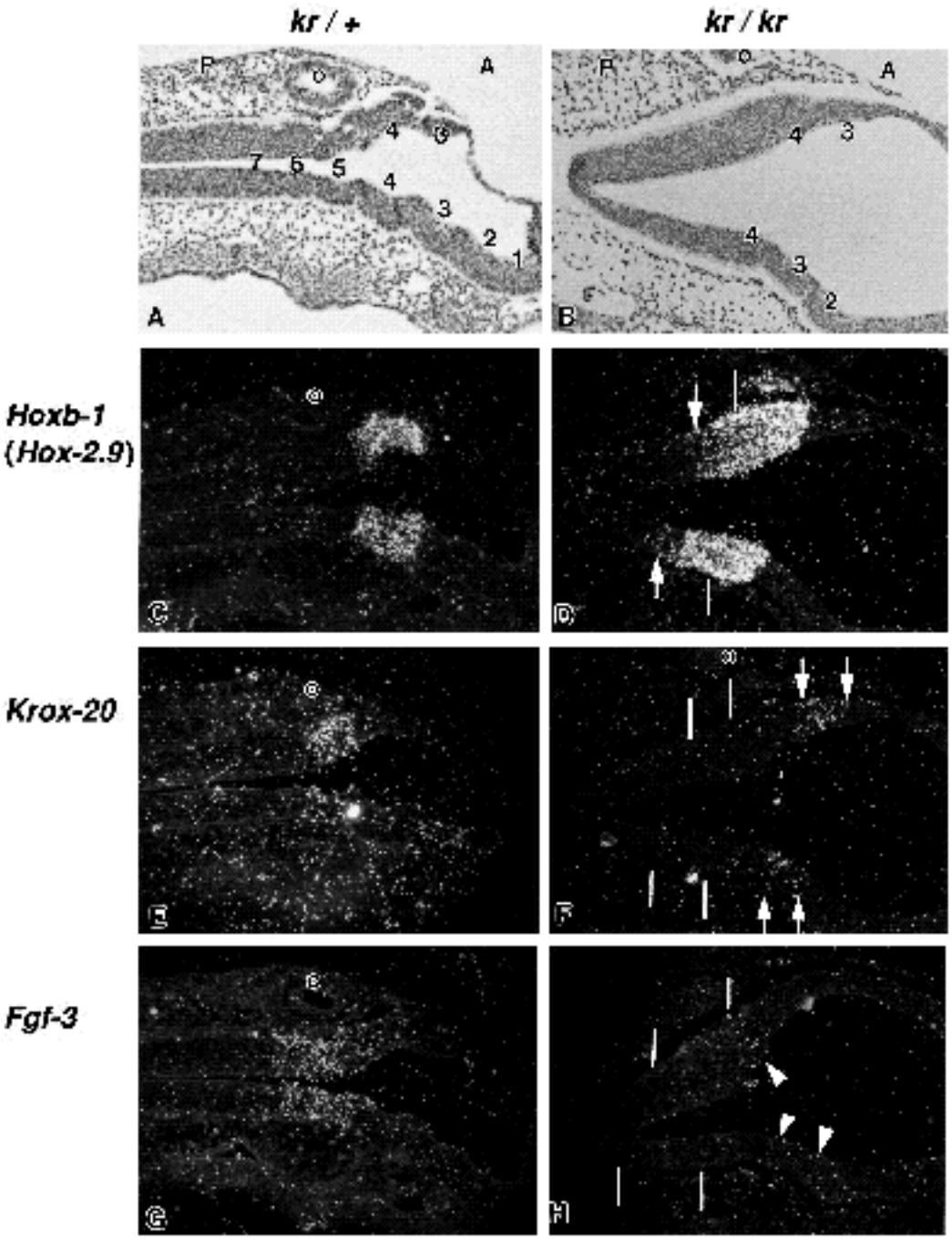

Fig. 3. Expression of *Krox-20* and *Fgf-3* genes in *kr*/+ and *kr*/*kr* embryonic hindbrains. The patterns of expression of the *Krox-20* and *Fgf-3* genes in the hindbrain of *kr*/+ and *kr*/*kr* embryos (E9.5) were determined by in situ hybridization of serial coronal sections. The bright-field images (A,B) are each representative of the set of serial sections hybridized with probes for *Hoxb-1* (C,D), *Krox-20*(E,F), and *Fgf-3* (G,H), shown beneath (dark-field images). Rhombomeres are numbered, except in the posterior part of the *kr*/*kr* hindbrain where rhombomere boundaries are not visible. Vertical bars indicate where the limit(s) of the normal expression domain would presumably be found, and vertical arrows indicate the limit of the abnormal *Hox* gene expression domain in *kr*/*kr* embryos. The arrowheads in H point to regions in which there are low levels of*Fgf-3* expression. A, anterior; nc, neural crest; o, otocyst; P, posterior. Magnification: ×80.

normal rhombomere-specific gene expression pattern, reflecting a disturbance in acquisition of positional identity.

The *Fgf-3* gene, a member of the FGF family of signalling molecules, is normally expressed in r5 and r6 (Wilkinson et al., 1988). The close temporal and spatial relationship between *Fgf-3* expression and the development of the otocyst has led to the suggestion that the *Fgf-3* gene product may be responsible for otic placode induction and/or subsequent otocyst differentiation (Wilkinson et al., 1988; Represa et al., 1991). As shown in Fig. 3G, *Fgf-3* RNA is detected in r5 and r6 in *kr*/+ embryos at E9.5. In contrast, we found that in the region corresponding to r5 and r6 of *kr*/*kr* embryos at the same stage of development, *Fgf-3* RNA was not detectable. Instead, patchy expression at very low levels was detected in more rostral structures, within the region corresponding to r4, in r3 and perhaps r2 (Fig. 3H and data not shown).

The morphology of the *kr*/+ and *kr*/*kr* hindbrain and the patterns of expression observed for *Hoxb-1, b-3, b-4, Krox-20,* and *Fgf-3* are summarized in Fig. 4. *Hoxb-1* and *Hoxb-4* display altered patterns of expression in a region of the neural tube that is morphologically abnormal in *kr*/*kr* embryos, caudal to where the r4/5 boundary would normally lie. However, *Hoxb-3*, *Krox-20*, and *Fgf-3* display altered patterns of expression rostral to the r4/5 boundary, a region that is morphologically normal in *kr*/*kr* embryos.

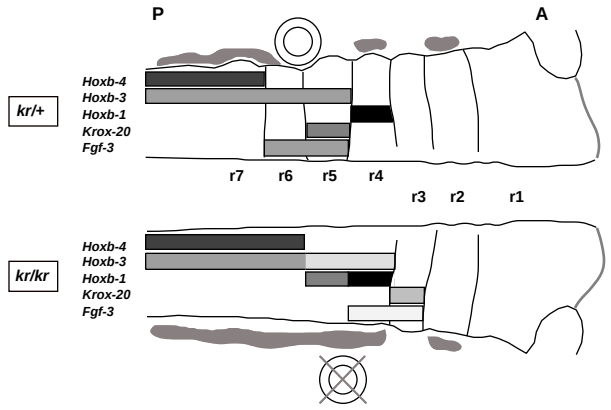

Fig. 4. Summary of gene expression in *kr*/+ and *kr*/*kr* hindbrains at E9.5. The upper part of the diagram illustrates half of a normal hindbrain, with rhombomeres 1-7 (r1-r7), the otocyst (concentric circles), and neural crest (shaded) adjacent to the regions from which it emigrates. The anterior limit of r1 is indicated by a dotted line, since it has not been shown to represent a lineage restriction boundary (Fraser et al., 1990). Domains of gene expression are represented by patterned horizontal bars. The lower part of the diagram illustrates half of an abnormally segmented *kr*/*kr* hindbrain. The preganglionic neural crest (shaded) is found in a continuous sheet extending caudally from the junction of r3 and r4, which separates the otocyst from the neural tube (Deol, 1964). The cross through the otocyst signifies that it does not develop normally. The *Hoxb-1* and *Hoxb-3* expression domains are represented in two tones to signify that the level of expression in *kr*/*kr* mice is not uniform across them. The *Fgf-3* and *Krox-20* expression domains are lightly patterned to indicate that expression is detected at low levels in *kr*/*kr* mice.

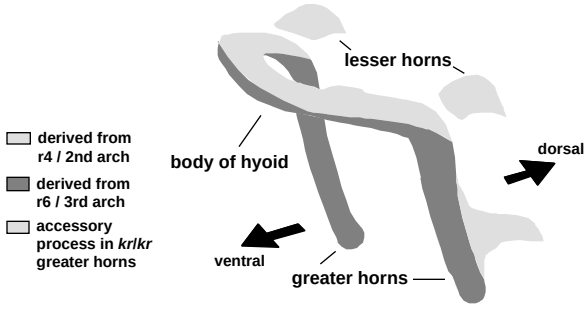

Fig. 5. Contributions of r4- and r6-derived neural crest to the adult hyoid bone. Based on grafting and dye-labelling studies in avian embryos, the lesser horns and the upper part of the body of the hyoid are derived from neural crest that originates in r4 and contributes to the second branchial arch. The lower part of the body and the greater horns of the hyoid are derived from neural crest that originates in r6 and contributes to the third branchial arch (Noden, 1978; Noden, 1988; Lumsden et al., 1991). The accessory process observed in *kr*/*kr* animals is indicated with a dotted line and projects dorsally, as do the lesser horns.

Abnormal differentiation of the hyoid bone in *kr*/*kr* mice

Neural crest cells that arise from different rhombomeres are thought to carry a form of prepatterning acquired during neural tube segmentation, which is later manifested, in part, by differentiation into specific bony and cartilaginous structures in the branchial arches (Noden, 1983, 1988; Lumsden et al., 1991). It has been suggested that *Hox* genes play some role in this prepatterning (Hunt et al., 1991b,c). We therefore investigated whether the altered patterns of *Hoxb* gene expression observed in the region representing r4, r5, and r6 of the *kr*/*kr* hindbrain might be associated with developmental abnormalities of the second and third branchial arches, which in +/+ embryos contain neural crest derived from r4 and r6, respectively.

Although abnormalities of the middle ear have been described thoroughly in *kr*/*kr* embryos and adults, most of these defects are positional deformities caused by abnormal development of the otic vesicle (Hertwig, 1944; Deol, 1964). For example, in *kr*/*kr* adults, the stapes, a middle ear bone derived from second arch neural crest, is often fused at its base and displaced into the cochlea. However, these abnormalities are probably due to cysts that develop from the *kr*/*kr* otic vesicle and later impinge on middle ear structures to produce secondary deformations (Deol, 1964). Thus, the pathology of the ears themselves reveals little concerning the nature of the initial developmental missteps. Therefore, as an indicator of primary malformations we chose to examine two other structures, the styloid and hyoid bones, which form from branchial arch neural crest derived from the region that is affected in *kr/kr* embryos, but whose development is not affected by that of the otic vesicle. In the adult, the styloid bone, which is derived from the second branchial arch, is located at the base of the skull, and the hyoid bone, which is derived from both the second arch (lesser horn of the hyoid) and third arch (greater horn of the hyoid), is located in the neck (Fig. 5; Horstadius, 1950; Noden, 1978, 1988; LeDouarin, 1980; Maderson, 1987; Morriss-Kay and Tan, 1987).

A total of 74 adult specimens (61 +/+, 5 *kr*/+, and 8 *kr*/*kr*)

Table 2. Hyoid morphology in *kr*/*kr*, *kr*/+, and +/+ animals

Mice*	No. examined	asymmetry of lesser horns†	asymmetry of greater horns†	accessory process on greater horn(s)
kr/*kr*	8	0	8 (100%)	8 (100%)
+/*kr*	5	0	3 (60%)	0
+/+	61	1 (2%)	2 (3%)	0

*Origin and genotype of the *kr*/*kr* and +/*kr* animals is described in Materials and Methods and Table 1. The +/+ specimens include 2 C3H/HeJ and 59 outbred mice (CD-1), none of which exhibited accessory processes on the hyoid greater horns. The tabulations include animals that were examined between E19.5 (when the accessory process first becomes apparent) and 12 months of age.

†Specimens were considered asymmetric if there were gross differences in shape or size of the lesser horns or greater horns when comparing one side to the other.

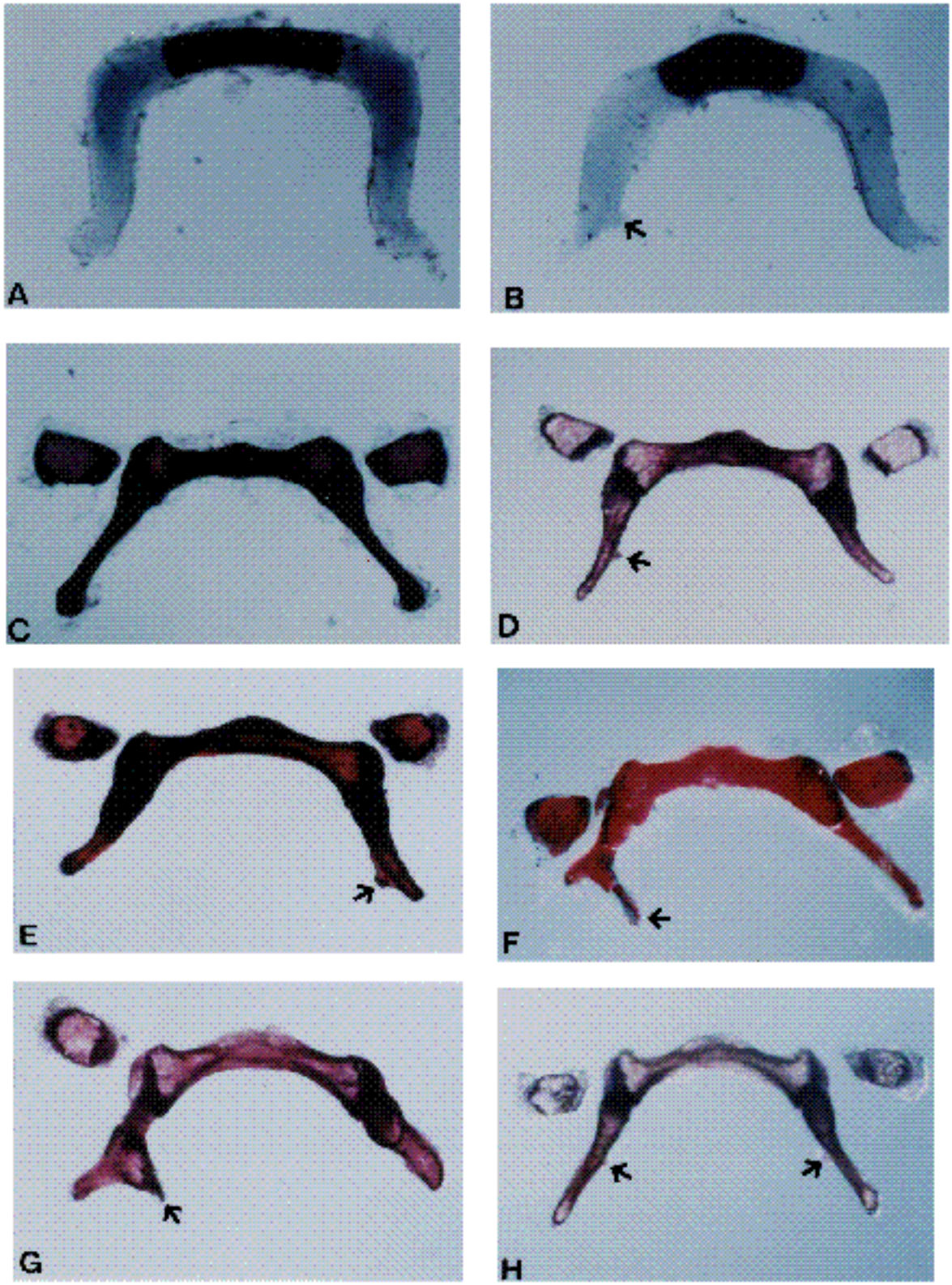

Fig. 6. Abnormal hyoid development in *kr*/*kr* animals. After dissection and removal of surrounding tissue, hyoid bones were stained with alcian blue and alizarin red (McLeod, 1980), and photographed at ×80 magnification under direct and reflected light. A and C show +/+ embryo (P0) and adult specimens, respectively. B and D show *kr*/*kr* embryo (E19.5) and adult specimens, respectively. E-H show specimens from different *kr*/*kr* adult animals treated with dilute proteinase K to remove residual connective tissue. The specimens in C, D, G, and H were photographed such that the lesser horns and accessory process project towards the viewer; the specimens in E and F were photographed such that the lesser horns and accessory process project away from the viewer. Accessory projections on the greater horn(s) of the hyoid in the *kr*/*kr* specimens are emphasized with arrows.

were examined by alizarin red/alcian blue staining of skeletal and cartilaginous structures (Table 2). There were no apparent effects of the kr mutation on the styloid bone or the lesser horn of the hyoid bone (data not shown). The most striking abnormalities observed in *kr*/*kr* animals were accessory projections present on the greater horns of the hyoid bone, seen in all of the postnatal *kr*/*kr* specimens, but in none of the +/+ and *kr*/+ specimens (Table 2, Fig. 6). In addition, the size and shape of the hyoid greater horn varied among *kr*/*kr* animals and between opposite sides in all mutant animals, whereas contralateral asymmetry of the hyoid greater horns was observed in *kr*/+ or +/+ specimens much less frequently (Table 2).

Examination of late gestation embryos, neonates, and juvenile animals revealed that the accessory projection first becomes apparent at E19.5 on the dorsal aspect of the hyoid greater horn (arrow, Fig. 6B). In every case, the accessory projection is directed dorsally, in the same direction as the hyoid lesser wing. This abnormality is quite specific, as no other laryngeal or tracheal cartilages are affected, and we have failed to find similar abnormalities in 61 +/+ or 5 *kr*/+ adult mice (Table 2). The accessory projection and subsequent stunting and/or clefting cannot be explained by an abnormal location or relationship of the hyoid to other developing structures. Instead, this combination of abnormalities is most easily explained by ectopic development of a second arch structure (the hyoid lesser horn) in an area that is normally formed by cells in the third arch (the hyoid greater horn; see Fig. 5).

DISCUSSION

The appearance of transiently segmented structures is a developmental feature shared by all vertebrates. Insights into the molecular mechanism of this process can be gained from analysis of mutations that perturb segmentation in the hindbrain. Here, we show that the *kr* mutation, which affects the metameric pattern of the developing rhombencephalon, disturbs the expression patterns of five genes expressed in the caudal hindbrain. *Hoxb-4*, *Hoxb-3*, *Krox-20* and *Fgf-3* exhibit rostral displacement of their domains of expression, whereas *Hoxb-1* exhibits an unusual disturbance in which the rostral limit of its expression domain appears normal but the caudal limit is extended. To determine if these abnormalities in gene expression patterns are correlated with abnormal differentiation of segment-derived adult structures, we examined bones derived from the neural crest of the second and third branchial arches in *kr*/*kr* adults. We found that the hyoid greater horn exhibits an accessory process that appears to have been derived by partial duplication of the hyoid lesser horn. We suggest that this abnormality arises from ectopic development of a second branchial arch structure in the third branchial arch.

Gene expression in the caudal hindbrain is restricted in the absence of rhombomere boundaries

The close temporal relationship between the onset of position-specific gene expression, the formation of rhombomere boundaries, and the restriction of cell lineage between adjacent rhombomeres has made it difficult to elucidate the order of these events in a developmental pathway (Wilkinson et al., 1989b; Fraser et al., 1990; Frohman et al., 1990; Sundin et al., 1990; Murphy and Hill, 1991). For example, an early step in hindbrain segmentation is the restriction of cell mixing between adjacent rhombomeres, which seems to occur simultaneously with the development of rhombomere boundaries (Fraser et al., 1990). However, it has been shown that there is position-specific expression of some genes (i.e. *Hoxb-1* and *Krox-20*) prior to boundary formation (Frohman et al., 1990; Murphy and Hill, 1991), indicating that the appearance of such boundaries represents a secondary event. In the caudal hindbrain of *kr*/*kr* mice, rhombomere boundaries do not develop, yet *Hoxb-4*, *Hoxb-3* and *Hoxb-1* all exhibit distinct limits of gene expression in the affected region. Furthermore, position-specific differentiation of caudal hindbrain derivatives is only slightly disturbed in *kr*/*kr* animals. Thus, formation of visible rhombomere boundaries is not required for the establishment of rostrocaudal differences in gene expression and differentiation. Similar observations have been made in two other situations. In E8.0 mouse embryos exposed to retinoic acid, rhombomere boundaries are not apparent, but *Hoxb-1* and *Krox-20* exhibit restricted, albeit abnormal, domains of expression (Morriss-Kay et al., 1991). Second, in mice homozygous for a targeted inactivation of *Hoxa-1 (Hox-1.6)*, rhombomere boundaries are not observed, yet neural crest-derived structures of the second and third branchial arches apparently develop normally (Chisaka et al., 1992).

It remains to be determined whether, in any of these situtations, the absence of visible boundaries represents an absence of functional boundaries; that is, whether the lack of rhombomere boundaries allows cells to mix abnormally. Evidence consistent with this idea is apparent from both our data and the studies of embryos exposed to retinoic acid. In *kr*/*kr* embryos, caudal extension of the *Hoxb-1* expression domain could be explained by absence of an r4/5 boundary if cells in the area of r4, which normally express *Hoxb-1* prior to rhombomere formation, mix abnormally with cells in the area of r5. Similarly, in embryos exposed to retinoic acid, abnormal cell mixing might account for expression of *Hoxb-1* and *Krox-20* in ill-defined alternating patches rather than distinct non-overlapping domains (Morriss-Kay et al., 1991). Moreover, during early stages of chick hindbrain development, expression of the protein encoded by *Ghox-lab* (chick *Hoxb-1* gene) exhibits an indistinct limit at the position of the future r3/4 boundary (Sundin et al., 1990). The limit becomes precise after the r3/4 boundary forms. Based on these observations, we speculate that formation of rhombomere boundaries in conjunction with restriction of cell mixing serves to sharpen the limits of gene expression, and thereby reinforces rather than initiates the steps that lead to rostrocaudal differences in differentiation.

Displacement of gene expression domains in *kr*/*kr* embryos

Although each gene that we have examined is affected differently by the *kr* mutation (summarized in Fig. 4), some general conclusions can be drawn. The rostral limits of *Hoxb-4* and *Hoxb-3* both appear to be shifted forward by

one rhombomere length. *Krox-20* expression is not detectable in r5 but low levels of RNA are present in r3, which is consistent with a forward shift of two rhombomere lengths at this stage of development. Similar results with respect to *Krox-20* expression, showing expression in r3 but not in r5 have been obtained by I. McKay and J. Lewis (personal communication). The alteration in *Fgf-3* expression is both qualitative and quantitative; a well-defined domain of expression in r5 and r6 is replaced by more rostral patches of expression at very low levels. Surprisingly, the altered patterns of *Hoxb-3*, *Krox-20*, and *Fgf-3* gene expression are not confined to the region of the neural tube that is morphologically abnormal. These data lead us to suggest that *kr* disturbs the rostrocaudal axis such that signals leading to position-specific gene expression are shifted forward from their normal position. Retinoic acid exposure also produces forward displacement of gene expression patterns and also of differentiated structures (Morriss-Kay et al., 1991; Papalopulu et al., 1991). However, it seems unlikely that *kr* affects establishment of a retinoid-induced gradient in a global fashion, because retinoic acid exposure has its most prominent effects on the preotic hindbrain, whereas *kr* affects the caudal hindbrain (Deol, 1964). Furthermore, abnormalities produced by retinoic acid exposure such as shortening of the forebrain and midbrain and rostral displacement of the somites (Morriss and Thorogood, 1978; Morriss-Kay et al., 1991) are not seen in *kr/kr* embryos.

The expression pattern of *Hoxb-1* is affected differently from those of the other genes we have examined, which may provide a clue to the time of *kr* gene action. In *kr*/*kr* embryos, the rostral limit of *Hoxb-1* expression is not shifted forward, but instead the caudal limit is extended. Normally, the rostral limit of *Hoxb-1* expression, which marks the site of the future r3/4 boundary, becomes established before overt rhombomere formation (Frohman et al., 1990; Sundin and Eichele, 1990; Murphy and Hill, 1991). By contrast, the rostral limits of *Hoxb-4* and *Hoxb-3* expression at r4/5 and r6/7, respectively, are established at or after rhombomere formation (Wilkinson et al., 1989b). These observations suggest that, in *kr*/*kr* embryos, rostrocaudal axis formation proceeds normally until after the position of the r3/4 boundary has been determined.

Relationship of *Fgf-3* expression to otocyst development

Transplantation experiments have demonstrated that induction of the otic pit and differentiation of the otic vesicle depend on position-specific signals emanating from the hindbrain (Yntema, 1933, 1950; Kaan, 1938; Zwilling, 1941; Ruben and Van De Water, 1983), and the normal temporal and spatial expression pattern of *Fgf-3* is consistent with a role in one or both of these inductive interactions (Wilkinson et al., 1988). In addition, there are data suggesting that interference with *Fgf-3* expression prevents normal otocyst formation (Represa et al., 1991). However, recent analysis of *Fgf-3*-deficient mice has demonstrated that this gene is involved in endolymphatic duct formation rather than earlier steps in ear development (Mansour et al., 1993). Our observations show that in *kr/kr* mice, *Fgf-3* is expressed at very low levels in an abnormally rostral domain. The lack of normal *Fgf-3* expression could account for the defects in otic vesicle differentiation in *kr/kr* mice, particularly the failure of normal endolymphatic duct formation.

Abnormal development of the hyoid bone in *kr*/*kr* animals

The accessory process present on the hyoid greater horn in *kr*/*kr* animals becomes apparent just before birth, but abnormalites are more readily detectable in adult mice. Our observations suggest that the accessory process does not represent a normal variant or a positional deformity caused by axial torsion or physical constraint, but instead is a malformation that represents ectopic development of a second arch structure, the hyoid lesser horn, in the area normally derived from the third branchial arch. This could represent a change in cell fate in which a caudal structure is partially transformed into a more rostral one. However, if expression of *Hox* genes in the hindbrain and in migrating neural crest plays a role in branchial arch patterning (Hunt et al., 1991c), then one might expect to find that their abnormal expression in more rostral domains would lead to the transformation of rostral to more caudal structures. Our data demonstrate that in *kr*/*kr* embryos the opposite pertains, such that a rostral structure (the hyoid lesser horn) is found in an abnormally caudal position. Perhaps *Hox* genes other than the ones we examined play a dominant role in branchial arch patterning. If so, the alterations of *Hoxb-4* and *Hoxb-3* expression we observed in the mutant hindbrain may not affect differentiation but, instead, simply indicate that position-specific signals responsible for branchial arch patterning are shifted rostrally. Paralogs from different *Hox* clusters generally exhibit similar domains of expression in the hindbrain (Hunt et al., 1991a), and it will be instructive to determine if this also applies to the *kr*/*kr* hindbrain. In addition, studies of *Hox* gene expression in the branchial arches of *kr*/*kr* embryos may help resolve whether the abnormal patterns of gene expression in the mutant hindbrain have resulted in a transformation of cell fate in the third branchial arch.

An alternative explanation for development of an ectopic lesser hyoid horn in the third branchial arch is based on the results of avian grafting experiments that showed that neural crest tissue is ‘prepatterned’ (Noden, 1983). In such studies, transplantation of first arch neural crest to the second arch resulted in the superimposition of first arch structures on second arch tissues (Noden, 1988). Thus, abnormal neural crest migration as an explanation for the morphologic abnormalities we observed in the hyoid bone would be consistent with histologic studies of *kr*/*kr* embryos (Deol, 1964). Normally, mesenchymal and preganglionic neural crest are derived only from even-numbered rhombomeres; discrete blastemata of preganglionic crest opposite r2, r4, and r6 give rise to the trigeminal, facial/acoustic, and glossopharyngeal/vagus ganglia, respectively (Noden, 1973; Lumsden and Keynes, 1989; Lumsden et al., 1991). Although the development of mesenchymal neural crest has not yet been described in *kr*/*kr* embryos, there is a continuous line of preganglionic neural crest opposite the caudal hindbrain and the facial/acoustic and glossopharyngeal/vagus ganglia are fused together (Hertwig, 1944; Deol,

1964). Therefore, abnormal mixing of mesenchymal neural crest in *kr*/*kr* embryos might allow 'predetermined' second arch neural crest to migrate into the third arch. Dye labelling of mesenchymal and/or preganglionic crest could be used to investigate the presence of such abnormal mixing.

Concluding remarks

Although the primary abnormality in *kr/kr* embryos appears to be one of hindbrain segmentation, the most obvious manifestations are in structures that lie outside of the central nervous system. It is possible that subtle patterning abnormalities are also present in caudal hindbrain derivatives**.** Such abnormalities have been described in mice homozygous for a targeted inactivation of *Hoxa-1*, where defects in rhombomere formation may be involved (Lufkin et al., 1991; Chisaka et al., 1992). Analysis of structures such as cranial nerve motor and brainstem nuclei in *kr*/*kr* embryos may reveal additional consequences of the early disturbances in hindbrain development.

The phenotypes of *kr*/*kr* embryos and adults, described some 25 and 50 years ago (Deol, 1964; Hertwig, 1944), provided evidence that a primary abnormality in neural tube segmentation could affect morphogenesis of the otic vesicle and cranial nerve ganglia. Our results have provided additional insight into how segmentation is perturbed by the *kr* mutation, but a detailed understanding of the molecular and developmental pathways involved will require isolation of the affected gene. Only a single *kr* allele exists, which because it was radiation-induced, may be associated with a large genomic deletion. However, recent advances in the techniques of genomic cloning, as well as in methods of experimental mutagenesis for generating additional alleles with small genomic changes (Justice and Bode, 1986; Rinchik et al., 1990), make it likely that *kr*, like other mouse developmental mutations, can be isolated on the basis of its genetic map position.

We thank Ian McKay and Julian Lewis for communicating their unpublished results on gene expression in *kr*/*kr* embryos, and Suzanne Mansour and Mario Capecchi for communicating their results regarding otocyst development in *Fgf-3*-deficient mice prior to publication. We are grateful to Gillian Morriss-Kay for extremely helpful comments on the manuscript. This work was supported by research grant HD-25331 to G. R. M. and by research grant HG-00377 from the National Institutes of Health to G. S. B. M. A. F. and S. P. C. were supported by fellowhips from the American Cancer Society. G. S. B. is an assistant investigator of the Howard Hughes Medical Institute.

REFERENCES

Chavrier, P., Zerial, M., Lemaire, P., Almendral, J., Bravo, R. and Charnay, P. (1988). A gene encoding a protein with zinc fingers is activated during G0/G1 transition in cultured cells. *EMBO J.* **7**, 29-35.

Chisaka, O., Musci, T. S. and Capecchi, M. R. (1992). Developmental defects of the ear, cranial nerves and hindbrain resulting from targeted disruption of the mouse homeobox gene *Hox-1.6*. *Nature* **355**, 516-520.

Davisson, M. T., Roderick, T. H. and Doolittle, D. P. (1989). Recombination percentages and chromosomal assignments. In *Genetic Variants and Strains of theLaboratory Mouse.* (ed. M. F. Lyon and A. G. Searle) pp. 432-505. Oxford: Oxford University Press.

Deol, M. S. (1964). The abnormalities of the inner ear in *kreisler* mice. *J. Embryol. Exp. Morph.* **12**, 475-490.

Fraser, S., Keynes, R. and Lumsden, A. (1990). Segmentation in the chick embryo hindbrain is defined by cell lineage restrictions. *Nature.* **344**, 431-435.

Frohman, M. A., Boyle, M. and Martin, G. R. (1990). Isolation of the mouse *Hox-2.9* gene: analysis of embryonic expression suggests that positional information along the anterior-posterior axis is specified by mesoderm. *Development* **110**, 589-607.

Frohman, M. A., Dush, M. K. and Martin, G. R. (1988). Rapid production of full-length cDNAs from rare transcripts: amplification using a single gene-specific oligonucleotide primer. *Proc. Natl. Acad. Sci. USA* **85**, 8998-9002.

Gaunt, S. J., Krumlauf, R. and Duboule, D. (1989). Mouse homeo-genes within a subfamily, *Hox-1.4*, *-2.6* and *-5.1*, display similar anteroposterior domains of expression in the embryo, but show stage- and tissue-dependent differences in their regulation. *Development* **107**, 131-141.

Graham, A., Papalopulu, N., Lorimer, J., McVey, J. H., Tuddenham, E. G. and Krumlauf, R. (1988). Characterization of a murine homeo box gene, *Hox-2.6*, related to the *Drosophila Deformed* gene. *Genes Dev.* **2**, 1424-1438.

Green, E. L. (1981). *Genetics and Probability in Animal Breeding Experiments.* New York: Oxford University Press.

Guthrie, S., Muchamore, I., Kuroiwa, A., Marshall, H., Krumlauf, R. and Lumsden, A. (1992). Neuroectodermal autonomy of *Hox-2.9* expression revealed by rhombomere transpositions. *Nature* **356**, 157-159.

Hertwig, P. (1942a). Neue Mutationen und Koppellungsgruppen bei der Hausmaus. *Z. indukt. Abstamm.-u. VererbLehre.* **80**, 220-246.

Hertwig, P. (1942b). Sechs neue Mutationen bei der Hausmaus in ihrer Bedeutung für allgemeine Vererbungsfragen. *Z. Lehre.* **26**, 1-21.

Hertwig, P. (1944). DieGenese der Hirn- und Gehörorganmissbildungen bei rontgenmurtierten Kreisler-Maüsen. *Z. KonstLehre.* **28**, 327-354.

Horstadius, S. (1950). *The Neural Crest.* London: Oxford University Press.

Hunt, P., Gulisano, M., Cook, M., Sham, M. H., Faiella, A., Wilkinson, D., Boncinelli, E. and Krumlauf, R. (1991a). A distinct *Hox* code for the branchial region of the vertebrate head. *Nature* **353**, 861-864.

Hunt, P., Whiting, J., Muchamore, I., Marshall, H. and Krumlauf, R. (1991b). Homeobox genes and models for patterning the hindbrain and branchial arches. *Development* **Supplement 1**, 187-196.

Hunt, P., Wilkinson, D. and Krumlauf, R. (1991c). Patterning the vertebrate head: murine *Hox 2* genes mark distinct subpopulations of premigratory and migrating cranial neural crest. *Development* **112**, 43-50.

Inouye, M. (1976). Differential staining of cartilage and bone in fetal mouse skeleton by alcian blue and alizarin red S. *Cong. Anom.* **16**, 171-173.

Justice, M. J. and Bode, V. C. (1986). Induction of new mutations in a mouse *t*-haplotype using ethylnitrosourea mutagenesis. *Genet. Res.* **47**, 187-192.

Kaan, H. W. (1938). Further studies on the auditory vesicle and cartilaginous capsule of *Amblystoma punctatum*. *J. Exp. Zool.* **78**, 159-183.

Keynes, R. and Lumsden, A. (1990). Segmentation and the origin of regional diversity in the vertebrate central nervous system. *Neuron* **2**, 1-9.

LeDouarin, N. (1980). Migration and differentiation of neural crest cells. *Current Top. Dev. Biol.* **16**, 32-86.

Lovett, M., Cheng, Z. Y., Lamela, E. M., Yokoi, T. and Epstein, C. J. (1987). Molecular markers for the *agouti* coat color locus of the mouse. *Genetics* **115**, 747-754.

Lufkin, T., Dierich, A., LeMeur, M., Mark, M. and Chambon, P. (1991). Disruption of the *Hox-1.6* homeobox gene results in defects in a region corresponding to its rostral domain of expression. *Cell* **66**, 1105-1119.

Lumsden, A. and Keynes, R. (1989). Segmental patterns of neuronal development in the chick hindbrain. *Nature* **337**, 424-428.

Lumsden, A., Sprawson, N. and Graham, A. (1991). Segmental origin and migration of neural crest cells in the hindbrain region of the chick embryo. *Development* **113**, 1281-1291.

Maderson, P. F. A. (1987). *Developmental and Evolutionary Aspects of the Neural Crest.* New York: John Wiley and Sons.

Mansour, S. L. and Martin, G. R. (1988). Four classes of mRNA are expressed from the mouse *int-2* gene, a member of the FGF gene family. *EMBO J.* **7,** 2035-2041.

Mansour, S. L., Goddard, J. M. and Capecchi, M. R. (1993). Mice homozygous for a targeted disruption of the proto-oncogene Int-2 have developmental defects in the tail and inner ear. *Development* **117**, 13-28**.**

McLeod, M. J. (1980). Differential staining of cartilage and bone in whole mouse fetuses by alcian blue and alizarin red S. *Teratology* **22**, 299-301.

Morriss, G. M. and Thorogood, P. V. (1978). An approach to cranial neural crest migration and differentiation in mammalian embryos. In

Development in Mammals. (ed. M. H. Johnson) pp. 387-400. Amsterdam: Elsevier North-Holland.

Morriss-Kay, G. M., Murphy, P., Hill, R. E. and Davidson, D. R. (1991). Effects of retinoic acid excess on expression of *Hox-2.9* and *Krox-20* and on morphological segmentation in the hindbrain of mouse embryos. *EMBO J.* **10**, 2985-2995.

Morriss-Kay, G. M. and Tan, S.-S. (1987). Mapping cranial neural crest cell migration pathways in mammalian embryos. *Trends Genet.* **3**, 257-262.

Murphy, P., Davidson, D. R. and Hill, R. E. (1989). Segment-specific expression of a homoeobox-containing gene in the mouse hindbrain. *Nature* **341**, 156-159.

Murphy, P. and Hill, R. E. (1991). Expression of the mouse *labial*-like homeobox-containing genes, *Hox 2.9* and *Hox 1.6* during segmentation of the hindbrain. *Development* **111**, 61-74.

Noden, D. M. (1973). An analysis of the migratory behavior of avian cephalic neural crest cells. *Dev. Biol.* **42**, 106-130.

Noden, D. M. (1978). The control of avian cephalic neural crest cytodifferentiation. I. Skeletal and connective tissues. *Dev. Biol.* **67**, 296-312.

Noden, D. M. (1983). The role of the neural crest in patterning of avian cranial skeletal, connective and muscle tissues. *Dev. Biol.* **96**, 144-165.

Noden, D. M. (1988). Interactions and fates of avian craniofacial mesenchyme. *Development* **103 Supplement**, 121-140.

Papalopulu, N., Clarke, J. D., Bradley, L., Wilkinson, D., Krumlauf, R. and Holder, N. (1991). Retinoic acid causes abnormal development and segmental patterning of the anterior hindbrain in *Xenopus* embryos. *Development* **113**, 1145-1158.

Represa, J., Leon, Y., Miner, C. and Giraldez, F. (1991). The *int-2* proto-oncogene is responsible for induction of the inner ear. *Nature* **353**, 561-563.

Rinchik, E. M., Carpenter, D. A. and Selby, P. B. (1990). A strategy for fine-structure functional analysis of a 6- to 11-centimorgan region of mouse chromosome 7 by high-efficiency mutagenesis. *Proc. Natl. Acad. Sci. USA* **87**, 896-900.

Ruben, R. J. and Van De Water, T. R. (1983). *Recent Advances in the Developmental Biology of the Inner Ear.* New York: Grune and Stratton.

Sham, M. H., Hunt, P., Nonchev, S., Papalopulu, N., Graham, A., Boncinelli, E. and Krumlauf, R. (1992). Analysis of the murine *Hox-2.7* gene: conserved alternative transcripts with differential distributions in the nervous system and the potential for shared regulatory regions. *EMBO J.* **11**, 1825-1836.

Siracusa, L. D., Buchberg, A. M., Copeland, N. G. and Jenkins, N. A. (1989). Recombinant inbred strain and interspecific backcross analysis of molecular markers flanking the murine *agouti* coat color locus. *Genetics* **122**, 669-679.

Siracusa, L. D., Russell, L. B., Jenkins, N. A. and Copeland, N. G. (1987). Allelic variation within the *Emv-15* locus defines genomic sequences closely linked to the *agouti* locus on mouse chromosome 2. *Genetics* **117**, 85-92.

Sundin, O. H., Busse, H. G., Rogers, M. B., Gudas, L. J. and Eichele, G. (1990). Region-specific expression in early chick and mouse embryos of *Ghox-lab* and *Hox-1.6*, vertebrate homeobox-containing genes related to *Drosophila labial. Development* **108**, 47-58.

Sundin, O. H. and Eichele, G. (1990). A homeo domain protein reveals the metameric nature of the developing chick hindbrain. *Genes Dev.* **4**, 1267-1276.

Tuckett, F., Lim, L. and Morriss-Kay, G. M. (1985). The ontogenesis of cranial neuromeres in the rat embryo. I. A scanning electron microscope and kinetic study. *J. Embryol. exp. Morph.* **87**, 215-228.

Tuckett, F. and Morriss-Kay, G. M. (1985). The ontogenesis of cranial neuromeres in the rat embryo . II. A transmission electron microscope study. *J. Embryol. exp. Morph.* **88**, 231-247.

Wilkinson, D. G., Bhatt, S., Chavrier, P., Bravo, R. and Charnay, P. (1989a). Segment-specific expression of a zinc-finger gene in the developing nervous system of the mouse. *Nature* **337**, 461-464.

Wilkinson, D. G., Bhatt, S., Cook, M., Boncinelli, E. and Krumlauf, R. (1989b). Segmental expression of *Hox-2* homoeobox-containing genes in the developing mouse hindbrain. *Nature* **341**, 405-409.

Wilkinson, D. G. and Krumlauf, R. (1990). Molecular approaches to the segmentation of the hindbrain. *Trends Neurosci.* **13**, 335-339.

Wilkinson, D. G., Peters, G., Dickson, C. and McMahon, A. P. (1988). Expression of the FGF-related proto-oncogene *int-2* during gastrulation and neurulation in the mouse. *EMBO J.* **7**, 691-695.

Yntema, C. L. (1933). Experiments on the determination of the ear ectoderm of *Amblystoma punctatum. J. Exp. Zool.* **65**, 317-357.

Yntema, C. L. (1950). An analysis of induction of the ear from foreign ectoderm in the salamander embryo. *J. Exp. Zool.* **113**, 211-244.

Zwilling, E. (1941). The determination of the otic vesicle in *Rana pipiens. J. Exp. Zool.* **86**, 333-342.

(Accepted 19 November 1992)